THE JOURNAL OF BIOLOGICAL CHEMISTRY VOL. 283, NO. 48, pp. 33447–33454, November 28, 2008

Assembly of Oligomeric Death Domain Complexes during Toll Receptor Signaling*

Received for publication, July 16, 2008, and in revised form, September 10, 2008 Published, JBC Papers in Press, October 1, 2008, DOI 10.1074/jbc.M805427200

Martin C. Moncrieffe[‡1], **J. Günter Grossmann**[§], **and Nicholas J. Gay**[‡]

From the [‡]*Department of Biochemistry, Cambridge University, Cambridge CB2 1GA and* [§]*Molecular Biophysics Group, School of Biological Sciences, University of Liverpool, Liverpool L69 7ZB, United Kingdom*

The *Drosophila* Toll receptor is activated by the endogenous protein ligand Spätzle in response to microbial stimuli in immunity and spatial cues during embryonic development. Downstream signaling is mediated by the adaptor proteins Tube, the kinase Pelle, and the *Drosophila* homologue of myeloid differentiation primary response protein (dMyD88). Here we have characterized heterodimeric (dMyD88-Tube) and heterotrimeric (dMyD88-Tube-Pelle) death domain complexes. We show that both the heterodimeric and heterotrimeric complexes form kidney-shaped structures and that Tube is bivalent and has separate high affinity binding sites for dMyD88 and Pelle. Additionally we found no interaction between the isolated death domains of Pelle and dMyD88. These results indicate that the mode of assembly of the heterotrimeric dMyD88-Tube-Pelle complex downstream of the activated Toll receptor is unique. The measured dissociation constants for the interaction between the death domains of dMyD88 and Tube and of Pelle and a preformed dMyD88-Tube complex are used to propose a model of the early postreceptor events in *Drosophila* Toll receptor signaling.

The bifunctional Toll pathway in *Drosophila* is indispensable for embryonic development and the innate immune response to Gram-positive bacteria and fungi (1). Toll is a Type I transmembrane receptor (2) whose architecture consists of N-terminal leucine-rich repeats, a transmembrane helix, and a C-terminal TIR[2] domain. It is activated by direct binding of the ligand Spätzle (3) that is cleaved from its inactive pro-form by the serine protease Easter during development (4) and by another serine protease, Spätzle-processing enzyme, during Toll-dependent antimicrobial and fungal responses (5). Activation of the Toll pathway during development sets in motion a series of events that culminate in the translocation of the Rel/NF-κB family member Dorsal into the nucleus and the activation of the zygotic genes *twist* and *snail* on the ventral side of the embryos and the deactivation of *zerknullt* and *decapentaplegic* on the dorsal side (6), whereas activation resulting from an immune challenge leads to the nuclear translocation of the Dorsal-related immunity factor (Dif) and the subsequent transcription of many genes including those encoding the antimicrobial peptides Drosomycin and Metchnikowin (7, 8). In mammals, an immune response is mounted as a result of challenge by a variety of pathogen-associated molecular patterns with the activation of a homologous Toll-like receptor pathway of which approximately 11 distinct members have been identified (9).

Signaling from the activated Toll receptor to the relevant transcription factors relies on interactions between adaptor proteins that associate with the TIR domain of Toll and subsequently influence interactions between other downstream components of the pathway. In *Drosophila*, the immediate post-receptor events are context-dependent; during an innate immune response, for example, the proteins involved are dMyD88, Tube, and Pelle (10), whereas an additional zinc finger adaptor, Weckle, is required for dorsoventral patterning of the embryo (11). These adaptors with the exception of Weckle all have an interaction motif belonging to the death domain (DD) superfamily, and additionally dMyD88 possesses a TIR domain (12) and Pelle a kinase domain (13). One model of the signal transduction events downstream of the Toll receptor posits that upon activation dimeric Toll recruits a membrane-localized dMyD88-Tube DD-DD heterodimer (14) via interactions between the TIR domains of Toll and dMyD88. This heterotrimeric complex then recruits Pelle, which undergoes autophosphorylation (15). Pelle then phosphorylates Toll and Tube (14) before being released from the complex. There is evidence that both Cactus and Dorsal are targets of activated Pelle (16, 17), and a possible scenario is that Pelle, or a currently unidentified kinase, phosphorylates Cactus, which releases Dorsal, and then Dorsal in turn is phosphorylated and enters the nucleus (18). An alternative model for the early events in the Toll pathway that was proposed before the role of dMyD88 was known suggests that a presignaling complex consisting of the TIR domain of Toll, Pelle, and Tube exists and that Spätzle binding and subsequent Toll dimerization results in the transphosphorylation of Pelle followed by the cascade of events as described previously (19).

From the preceding, DD-DD interactions are crucial for the transduction of the signal from the activated Toll receptor. The canonical death domain revealed initially by the NMR solution

* This work was supported by a project grant from the UK Biotechnology and Biological Sciences Research Council (BBSRC) (to N. J. G.). The costs of publication of this article were defrayed in part by the payment of page charges. This article must therefore be hereby marked "*advertisement*" in accordance with 18 U.S.C. Section 1734 solely to indicate this fact.

[1] To whom correspondence should be addressed: Dept. of Biochemistry, University of Cambridge, 80 Tennis Ct. Rd., Cambridge CB2 1GA, UK. Fax: 44-1-223-766002; E-mail: mcm35@cam.ac.uk.

[2] The abbreviations used are: TIR, Toll-interleukin receptor; DD, death domain; SAXS, small angle x-ray scattering; dMyD88, *Drosophila* homologue of MyD88; CARD, caspase recruitment domain; FADD, Fas-associated protein with a death domain; PIDD, p53-induced protein with a death domain; RAIDD, receptor-interacting protein (RIP)-associated ICH-1/CED-3 homologous protein with a death domain; R_g, radius of gyration; r.m.s.d., root mean square deviation; D_{max}, maximum molecular dimension.

structure of the Fas DD has a six-helix bundle fold (20, 21). Three-dimensional structures of the heterodimeric Pelle-Tube DD-DD (22) and the CARD-CARD Apaf-1-Procaspase-9 complexes have been solved crystallographically. On the basis of the different interactions comprising the interface of these structures and the interactions obtained by superimposing Pelle onto Procaspase-9 of the Apaf-1-Procaspase-9 complex, three types of interactions were defined. Type I interactions, typified by the CARD-CARD interface, involve charge-charge contacts between the second and third helices of Apaf-1 and the first and fourth helices of Procaspase-9. Type II interactions are observed in the Pelle-Tube DD interface in which helix 4 of Pelle interacts with a groove formed by three helices (helices 1, 2, and 6) of Tube, and the C-terminal tail of Tube interacts with a groove on Pelle created by helices 2, 3, and 5. Type III interactions are a combination of Type I and Type II and are characterized by contacts between helix 3 of Apaf-1 with the loops between the first and second helices and third and fourth helices of Tube (23). Additionally a docking model of the Fas-FADD DD revealed that a hexameric complex was possible implying that death domains have the potential for forming multivalent interactions (24). This prediction has been substantiated by the only oligomeric DD-DD structure to date, the PIDD-RAIDD complex (25). This asymmetric complex consists of five PIDD and seven RAIDD molecules, and the interactions at the different interfaces belong to the three types described previously (24) suggesting that such interactions may be sufficient to define the assembly of DD-DD complexes.

Regarding the DD complexes involved in Toll signaling, solution data (26, 27) strongly suggest a 1:1 interaction between Pelle and Tube. The crystal structure of the Pelle-Tube complex, although prepared from a heterodimeric DD solution, revealed a tetramer in the asymmetric unit consisting of two Pelle-Tube heterodimers arranged in a linear array (P1:T1:P2:T2) (22). We have suggested, given the bivalent nature of the Tube DD, that the T1:P2 interface observed crystallographically may be the binding site for other members of the complex.

In the present study we used a variety of biophysical techniques including analytical ultracentrifugation, isothermal titration calorimetry, and small angle x-ray scattering to probe the nature and affinity of the DD complexes involved in postreceptor Toll signaling. We suggest a model for the immediate postreceptor events.

EXPERIMENTAL PROCEDURES

Sample Preparation—The expression and purification of Pelle DD and Tube DD has been described previously (27). The expression and purification of the death domain of *Drosophila* MyD88 was similar to that of Pelle DD and Tube DD with the exception that protein expression was done using Rosetta (Novagen) cells. The MyD88-Tube DD complex was formed by adding a slight molar excess of dMyD88 DD to purified Tube DD, and the resulting protein solution was concentrated and loaded onto a Superdex-75 (Amersham Biosciences) size exclusion column and eluted with 20 mM Tris, 20 mM NaCl, 5 mM dithiothreitol, pH 7.5. The heterotrimeric Pelle-Tube-MyD88 DD complex was made by adding excess purified Pelle DD to purified dMyD88-Tube DD. For small angle x-ray scattering (SAXS) measurements excess Pelle DD was removed using a Superdex-75 size exclusion column as done before for the dMyD88-Tube complex.

Analytical Ultracentrifugation—Sedimentation equilibrium and sedimentation velocity measurements were performed using a Beckman XL-A analytical ultracentrifuge equipped with absorbance and interference optics. Sedimentation equilibrium experiments on the dMyD88-Tube complex were performed using 180-μl sample volumes and three concentrations (0.04, 0.02, and 0.01 mg/ml obtained by serial dilution of a solution obtained as a single peak from a size exclusion column). This provided a powerful constraint in data analysis as the ratio of the concentrations of Tube and dMyD88 was fixed at 1.0. Absorption (230 and 280 nm) and interference data were acquired at three rotor speeds (13,000, 19,000, and 25,000 rpm) using an An60-Ti (Beckman Coulter) rotor after the time taken for the attainment of equilibrium (48 h) at each speed. The molar absorptivities of Tube and dMyD88 DD at 230 and 280 nm were determined using the Edelhoch (28) method. Partial specific volumes, buffer density, and viscosity were calculated using SEDNTERP, and the data were analyzed with SEDPHAT (29). Sedimentation equilibrium experiments were also performed using protein concentrations of 0.1 mg/ml for both the dMyD88-Tube and the dMyD88-Tube-Pelle complexes. Sedimentation velocity data for the Tube-dMyD88 (0.1 mg/ml) DD complex and a mixture of the Pelle and dMyD88 (0.2 mg/ml) death domains were obtained using a rotor speed of 60,000 rpm and the interference optical system. Typically 100 scans were acquired every 2 min, and the data were analyzed using the program SEDFIT (30).

Isothermal Titration Calorimetry—The association constants characterizing the binding of Tube to dMyD88 and of Pelle DD to a Tube-dMyD88 complex were obtained from measurements made on a Microcal VP-ITC microcalorimeter at 20 °C. Protein concentrations for the Tube-dMyD88 interaction were 5 and 50 μM and for Pelle binding to Tube-dMyD88 were 4.86 (Pelle) and 119 μM. Data were reduced using the Origin software package and then analyzed using SEDPHAT (31).

SAXS—X-ray scattering data of the Tube-dMyD88 and Pelle-Tube-dMyD88 complexes in solution were collected at 4 °C at the Synchrotron Radiation Source (Daresbury, UK) using sample-to-detector distances of 1 and 4.5 m. Protein concentrations ranged between 2.5 and 10 mg/ml for the Tube-dMyD88 complex and 2.5 and 5 mg/ml for the Pelle-Tube-dMyD88 complex. The scattering data at both detector distances for each sample were merged, and the Fourier transform method implemented in the program GNOM (32) was used to calculate the radius of gyration (R_g) and the maximum molecular dimension (D_{max}) via the distance distribution function $P(r)$. The scattering profiles were then used in *ab initio* shape restorations using the program GASBOR (33). Eighty independent shape reconstructions were performed for each complex assuming no symmetry constraints. The resulting shapes were then aligned, averaged, and filtered using the DAMAVER (34) and SUPCOMB (35) packages. Docking of the high resolution Pelle-Tube DD structure (Protein Data Bank code 1D2Z) into

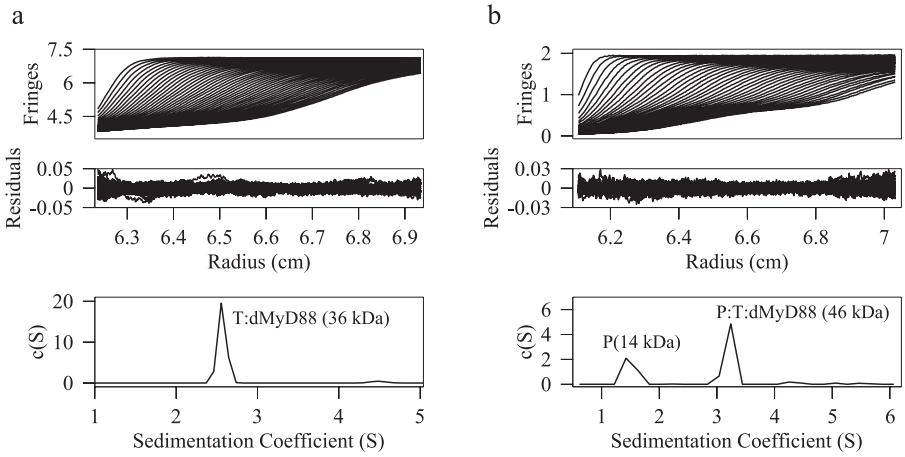

FIGURE 1. **Sedimentation velocity profiles, the residuals after fitting, and the *c*(*S*) distribution for the dMyD88-Tube (*a*) and the Pelle-Tube-dMyD88 (*b*) death domain complexes.** The sedimentation coefficient of the heterodimeric complex was 2.55 S, and the recovered molecular mass was 36 kDa, whereas for the heterotrimeric complex the sedimentation coefficient was 3.24 S, and the molecular mass was 46 kDa. The peak at 1.42 S (*b*) is due to excess Pelle DD. *P*, Pelle; *T*, Tube.

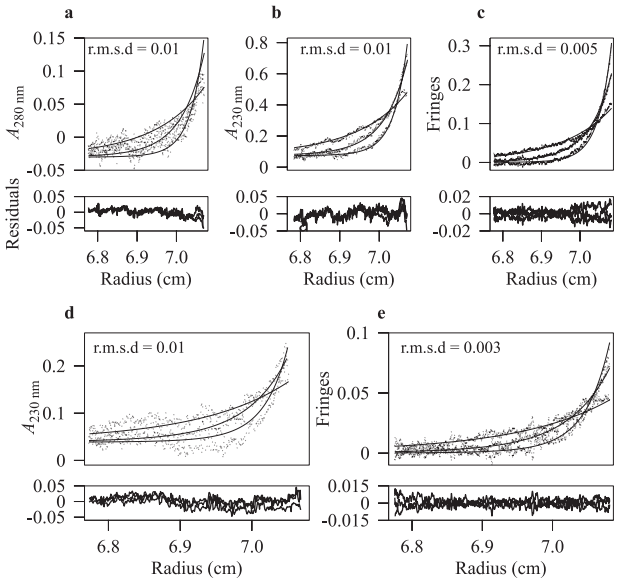

FIGURE 2. **Sedimentation equilibrium profiles of the dMyD88-Tube death domain complex.** Shown are interference (*c* and *e*) and absorbance data at 280 (*a*) and 230 nm (*b* and *d*) that were acquired at rotor speeds of 13,000, 19,000, and 25,000 rpm and sample concentrations of 0.04 (*a*–*c*) and 0.02 mg/ml (*d* and *e*). Data were analyzed with global implicit mass conservation constraints, and the local r.m.s.d. of each fit is shown in the corresponding plot. The residuals after fitting are shown *below* the exponential curves for each panel.

the low resolution SAXS model was performed using the SITUS suite of programs (36, 37).

RESULTS

The Tube-dMyD88 DD Complex Is Stable—Tube and dMyD88 each contain a DD, a structural motif that associates via homotypic interactions in which DD-DD interactions are formed exclusively. Immunoprecipitation experiments revealed a substantial interaction between the death domains of Tube and dMyD88 (10). To determine the oligomeric state of the Tube-dMyD88 DD complex we performed sedimentation velocity experiments on a solution of these proteins obtained as a single peak from a Superdex-75 (Amersham Biosciences) size exclusion column. Fig. 1*a* shows the experimental profiles; the sedimentation coefficient distribution, *c*(*S*); and the residuals obtained after fitting the data with SEDFIT (30). The r.m.s.d. of the fit was 0.005, and the recovered frictional coefficient was 1.49. The *c*(*S*) distribution shows a single peak at 2.55 S corresponding to a molecular mass of 36 kDa. The recovered molecular mass is within 3% of the molecular weight calculated from the sequence assuming a 1:1 DD-DD complex. The molecular weight obtained from the sedimentation velocity experiments was confirmed by sedimentation equilibrium experiments (Fig. 2) performed on multiple concentrations of the complex and three rotor speeds. Additionally sedimentation equilibrium measurements performed on higher concentrations (0.1 mg/ml) yielded results identical to those at low concentrations and to that obtained from analysis of the sedimentation velocity data. The sedimentation coefficient of the Pelle-Tube DD complex (27) was 2.54 S, which, within experimental error, is identical to that of the Tube-dMyD88 complex suggesting that the shape adopted by these heterodimers is similar. The hydrodynamic radius of the Tube-dMyD88 complex calculated from the value of the sedimentation coefficient is 3.37 nm. If the complex is modeled as an oblate spheroid having a degree of hydration of 0.4 mg/ml, the maximum linear dimension is 9.8 nm, whereas for a prolate spheroid the value is 17.3 nm.

dMyD88 Binds Tube with High Affinity—Having established that the isolated death domains of dMyD88 and Tube form a stable complex in solution we sought to determine the strength of the association. The only published data detailing the strength of the interaction between death domain complexes is that of Schiffman *et al.* (26) who reported a K_d value of 0.64 μM for the interaction between an N-Tube (residues 1–257) and N-Pelle (residues 1–208) DD construct. The measured K_d obtained using isothermal titration calorimetry for the Pelle-Tube DD complex used in the present work was 0.5 μM (data not shown), which is similar to that obtained for the larger complex. An estimate of the K_d for the interaction between the death domains of Tube and dMyD88 was obtained from sedimentation equilibrium data collected at three concentrations and utilizing multiple rotor speeds and optical detection methods. Data were analyzed with global implicit mass conservation constraints as implemented in the program SEDPHAT (29). Fig. 2 shows the sedimentation equilibrium profiles obtained for two concentrations (0.04 and 0.02 mg/ml) of the Pelle-Tube DD complex and the local r.m.s.d. of the fits. The data are of excellent quality, and the K_d value obtained was 32 nM. To evaluate the reliability of the recovered K_d values, F-statistics and the error surface projection method implemented in SEDPHAT were used to calculate the critical χ^2 value; the K_d values

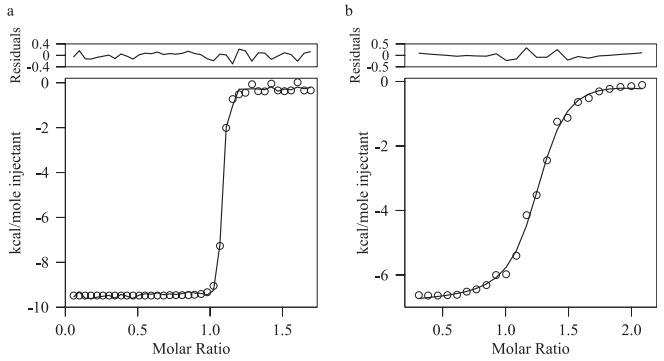

FIGURE 3. **Isothermal titration calorimetry of the interactions between the death domains of Tube and dMyD88 (*a*) and between the death domains of Tube-dMyD88 DD and Pelle (*b*).** The data after subtraction of the buffer control are shown (○) as are the fit to a single site model and the resulting residuals.

were then subsequently fixed at successively non-optimal values, and the χ^2 was recalculated. This analysis suggested that the K_d value of 32 nM obtained was an upper limit and that the binding was likely to be stronger. To obtain a more accurate estimate for the strength of the interaction between the death domains of dMyD88 and Tube we used isothermal titration calorimetry. Fig. 3*a* shows the binding isotherm fitted to a single site model in SEDPHAT (31). The K_d value obtained from this analysis was 1.2 nM with a ΔH value of −8.98 kcal/mol and a stoichiometry of 1:1.2. Thus, the interaction between the death domains of dMyD88 and Tube is of very high affinity and is greater, by more than 2 orders of magnitude, than that between the death domains of Tube and Pelle.

Pelle DD Binds to the dMyD88-Tube DD Complex with High Affinity—The heterotrimeric complex comprising the Pelle, Tube, and dMyD88 death domains was obtained by adding a slight excess of purified Pelle DD to a purified preexisting Tube-dMyD88. Sedimentation velocity measurements were performed on the resulting solution to confirm the presence of the heterotrimer. The *c*(*S*) distribution (Fig. 1*b*) obtained from an analysis of this data shows two peaks at 1.42 and 3.24 S. The corresponding molecular masses from a *c*(*M*) analysis were 14 and 46 kDa, which are within 9 and 8% of the molecular weights calculated from the sequence of the Pelle DD and the Pelle-Tube-dMyD88 death domains, respectively. The molecular weight of the dMyD88-Tube-Pelle complex was also confirmed using sedimentation equilibrium experiments (data not shown) and is, within experimental error, identical to that derived from the sedimentation velocity data. The r.m.s.d. of the fit was 0.005, and the value of the frictional coefficient was 1.42. The hydrodynamic radius of the heterotrimeric Pelle-Tube-dMyD88 complex, calculated from the sedimentation coefficient value is 3.55 nm. The maximum linear dimension for a prolate and oblate spheroid assuming a degree of hydration of 0.4 mg/ml were 16.85 and 10 nm, respectively. The dissociation constant for the interaction between Pelle DD and the Tube-dMyD88 death domain complex was determined by isothermal titration calorimetry (Fig. 3*b*). Data were fitted to a single site model and the K_d value obtained was 51 nM, and ΔH was −9.54 kcal/mol. Thus, the binding of Pelle DD to the Tube-MyD88 DD complex is cooperative and is enhanced approximately

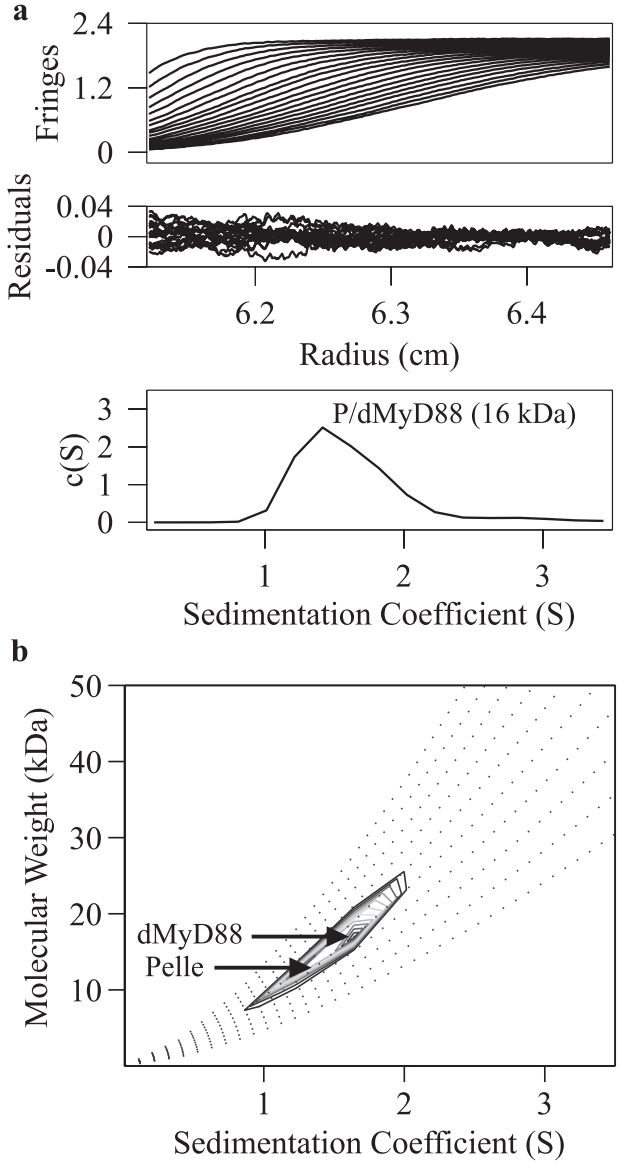

FIGURE 4. **Sedimentation velocity profiles of solution containing a mixture of the Pelle and dMyD88 death domains.** Data analysis with a *c*(*S*) distribution yields a sedimentation coefficient of 1.41 (*a*) and molecular mass from a *c*(*M*) analysis of 16 kDa. The *c*(*s*,*f*$_r$) analysis (*b*) indicates two components having molecular masses of ~12 and 16 kDa corresponding to the death domains of Pelle (*P*) and dMyD88, respectively.

12-fold relative to the binding of the isolated Pelle DD to the DD of Tube.

No Interaction between the Pelle and dMyD88 Death Domains—An interaction between the death domains of dMyD88 and Pelle has been implied by several studies (12, 38). We used sedimentation velocity to assess the extent of the interaction between these death domains *in vitro*. Fig. 4*a* shows the experimental sedimentation profiles of a solution containing a mixture of Pelle and dMyD88 death domains and the *c*(*S*) distribution after fitting. The peak in the *c*(*S*) distribution is at 1.41 S, which corresponds to a molecular mass of 16 kDa. The recovered frictional coefficient was 1.59, and the r.m.s.d. of the fit was 0.009. The *c*(*S*) analysis assumes that all sedimenting particles have the same weight average frictional coefficient, a condition that may not be valid for the Pelle and dMyD88 death

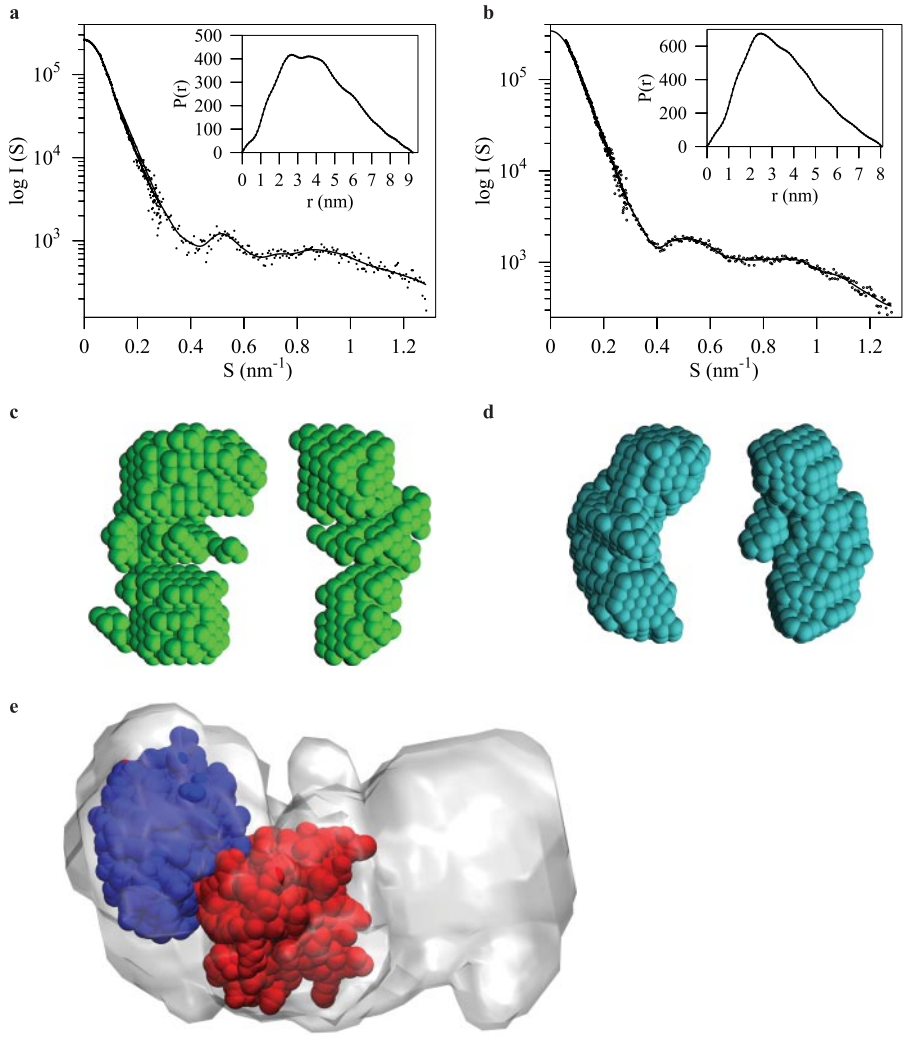

FIGURE 5. X-ray scattering profiles of the Pelle-Tube-dMyD88 death domain heterotrimer (*a*) and the Tube-dMyD88 death domain heterodimer (*b*) are shown (S=2 Sin(θ)/λ, where θ is the scattering angle and λ the wavelength 0.154 nm). The *inset* shows the distance distribution functions for both complexes from which maximum particle dimensions of 9.2 (heterotrimer) and 8.0 nm (heterodimer) are obtained. Two orthogonal orientations of the *ab initio* models of the heterotrimeric (*c*) and the heterodimeric (*d*) complex are shown. The superimposition of the SAXS-derived model of the Pelle-Tube-dMyD88 heterotrimer with the high resolution x-ray structure of the Pelle-Tube death domain heterodimer (*e*) is shown. The Tube death domain is colored *red*.

domains. A subsequent two-dimensional analysis, $c(s,f_r)$ (39), was performed in which this scaling restriction is lifted. The r.m.s.d. from the $c(s,f_r)$ analysis was 0.006, and the peak in the $c(S)$ distribution appears to have two components having molecular masses of ~12 and 16 kDa (Fig. 4*b*). These data show that the death domains of Pelle and dMyD88 do not interact.

Pelle-Tube-dMyD88 Heterotrimer Displays a Kidney-shaped Conformation—The structures adopted by the Tube-dMyD88 DD complex or the heterotrimeric Pelle-Tube-dMyD88 DD complexes are not known. Regarding the Tube-dMyD88 DD interaction, it has been shown that two mutations, K87E and R126E, in the Tube DD prevent formation of the Tube-dMyD88 DD complex (14). Although these residues are on a surface that is opposite to the sites of interaction between the Pelle-Tube DD (P1:T1) there are no structural data to exclude the possibility that in the heterotrimeric Pelle-Tube-dMyD88 DD complex dMyD88 binds in a manner that bridges the Pelle-Tube DD. Information about the shapes adopted by the heterodimeric dMyD88-Tube and the heterotrimeric Pelle-Tube-dMyD88 DD complexes was obtained from small angle scattering data collected over a wide angular range (Fig. 5, *a* and *b*). The value for R_g, an indicator of molecular compactness, for the Tube-dMyD88 complex is 2.68 ± 0.01 and 3.12 ± 0.01 nm for the Pelle-Tube-dMyD88 trimer. For comparison, the theoretical R_g value for the Pelle-Tube DD complex, based on its crystal structure (Protein Data Bank code 1D2Z), is 2.1 nm. Because Tube (20.5 kDa) is the common component of the Pelle-Tube and Tube-dMyD88 complexes, the larger R_g value of the Tube-dMyD88 complex is likely to be a reflection of the increased mass of dMyD88 (16.7 kDa) relative to Pelle (12.6 kDa) resulting in an extension at the periphery of the Tube-dMyD88 complex relative to the crystallographic Pelle-Tube structure.

The distance distribution functions, $P(r)$ (see Fig. 5, *a* and *b*, *insets*), confirm the size differences between the Tube-dMyD88 and Pelle-Tube-dMyD88 complexes. The $P(r)$ function provides an estimate of the D_{max} of both complexes, and these values are 8.0 ± 0.5 and 9.2 ± 0.5 nm for the Tube-dMyD88 and Pelle-Tube-dMyD88 complexes, respectively. The SAXS data suggest that there is limited flexibility between the constituent monomer protein cores; this is expected in view of the high affinity interaction between the Tube-dMyD88 and Pelle-Tube-dMyD88 complexes.

For visualization of the three-dimensional conformation of the Tube-dMyD88 heterodimer and the Pelle-Tube-dMyD88 heterotrimer *ab initio* shape reconstructions of the Tube-dMyD88 heterodimer and the Pelle-Tube-dMyD88 heterotrimer were performed on the basis of the SAXS data (see Fig. 5, *c* and *d*). Although both models can be described as having kidney-shaped structures, there are differences in the curvature and shape of the cleft in both models. These models also suggest that the binding of Pelle DD to the Tube-dMyD88 DD complex occurs on the larger of the two domains (Tube) seen in the Tube-dMyD88 complex. The SAXS bead model of the Pelle-Tube-dMyD88 heterotrimer was converted into a volumetric map, and rigid body docking of the Pelle-Tube DD heterodimer was performed using the six-dimensional search and filtering methodology implemented in the CoLoRes program (36). This docking procedure revealed that dMyD88 binds to the opposite side of

Pelle on Tube to form an almost linear Pelle-Tube-dMyD88 death domain heterotrimer (Fig. 5*e*).

DISCUSSION

Information transfer via Toll and the homologous Toll-like receptor pathway requires the recruitment of adaptor molecules that associate with the TIR domain of these receptors and propagate the signal to downstream components. In *Drosophila* a core set of adaptors, dMyD88, Tube, and Pelle, constitute the immediate postreceptor molecules involved in both development and the response to infection. In mammals, the Toll-like receptor pathway utilizes four other adaptors in addition to a direct homolog of dMyD88 (40). The association of dMyD88, Tube, and Pelle into a heterotrimeric signaling complex results from homotypic interactions involving their death domains, and we used biophysical methods to characterize the strength of these interactions and to probe the structures adopted by these death domain complexes.

The K_d values obtained calorimetrically (1.2 nM) and from sedimentation equilibrium analysis (32 nM) reveal that the binding of the death domains of Tube and dMyD88 is a very high affinity interaction. These data rationalize the finding that prior to signaling through Toll dMyD88 is found as a complex with Tube (14). Unexpectedly given the measured K_d value for the interaction between the isolated death domains of Tube and Pelle (26), we found that the binding of Pelle to a preformed Tube-dMyD88 complex resulted in 12-fold enhancement of the binding affinity. This implies that the binding of Pelle DD to the dMyD88-Tube DD complex is cooperative and additionally that either the Tube-Pelle interface has changed relative to that observed crystallographically or that the binding of dMyD88 to Tube affects the dynamics of the residues involved in Tube DD binding to the Pelle DD. The implications of the high affinity interaction between Pelle DD and the dMyD88-Tube DD complex with regard to Toll signaling will be discussed.

There are conflicting reports regarding the composition of the putative presignaling complex. A model of Toll signaling (19) suggests that Pelle (in association with Tube) interacts with Toll (15, 19) or is membrane-localized prior to Toll activation. Spätzle binding and the resulting dimerization of Toll results in a high local concentration of Pelle that leads to its activation by transphosphorylation. Activated Pelle phosphorylates Toll and Tube, is released, and phosphorylates downstream components. Sun *et al.* (14), however, found that dMyD88 directs Tube membrane localization and that the dMyD88-Tube complex preferentially binds to activated Toll. The mechanism by which the dMyD88-Tube complex is localized to the membrane is unknown. Recent reports have shown that myristoylation of the TIR-domain-containing adapter-inducing interferon-β-related adaptor molecule (41) and a phosphatidylinositol 4,5-bisphosphate binding domain on TIR domain-containing adapter protein (42) allows membrane recruitment, and consequently there may be an unidentified molecule in *Drosophila* or a sequence in dMyD88 that performs a similar function. By using co-transfection assays Sun *et al.* (14) also noted that the recruitment of Pelle into a Tube-dMyD88 complex resulted in Pelle autophosphorylation. Although the observed autophosphorylation could be a result of the concentrations of Pelle used in these assays, and thus independent of trimer formation, it was postulated that the presignaling complex is devoid of Pelle and that the recruitment of Pelle to Toll occurs after formation of the heterotrimeric Toll-dMyD88-Tube complex. Our finding of a high affinity interaction between the death domains of Pelle and Tube when Tube DD is already bound to dMyD88 DD suggests that death domain interactions are entirely sufficient to drive assembly of the heterotrimeric presignaling complex immediately downstream of Toll. Additionally specificity of heterotrimer assembly is guaranteed by ensuring that both Pelle and dMyD88 interact only with Tube and not with each other.

Although *Drosophila* and human MyD88 are homologues there are significant differences in the way that they function. Notably unlike dMyD88, hMyD88 is not localized to the membrane in unstimulated cells. A sequence alignment of the two proteins reveals that residues required for recruitment of MyD88 by both Tube and Toll are only partially conserved. Additionally there are extensions at both the N and C termini of dMyD88 that have low sequence complexity and thus may not form a fixed tertiary structure. The C-terminal extension in particular is highly basic and could serve a function similar to that of the N-terminal region of the human Mal adaptor to localize MyD88 to the membrane by interacting with phosphoinositides or other phospholipids (42, 43). The results presented here also show that the dMyD88-Tube dimer binds constitutively to Pelle in solution with high affinity. In the embryo, however, it appears that the concentration of the heterotrimeric dMyD88-Tube-Pelle complex is small or alternatively that the dMyD88-Tube heterodimer is unable to bind Pelle in the unstimulated condition suggesting that membrane localization sequesters the interaction site for Pelle on the Tube death domain. Thus, there are two plausible models of signal transduction. The first is that the membrane-associated dMyD88-Tube heterodimer is released or reoriented as a result of interactions between the TIR domains of dMyD88 and activated Toll. This event unmasks the binding site on Tube for Pelle allowing its recruitment into the postreceptor complex and initiating downstream signaling (see Fig. 6). Alternatively a membrane-localized dMyD88-Tube-Pelle complex (Fig. 6*c*) could bind to the activated Toll such that transphosphorylation of the kinase domains of Pelle and subsequently other downstream signaling events occur.

Another distinct property of hMyD88 is that it is constitutively dimeric with its dimerization mediated by the death domains.[3] In the absence of a vertebrate Tube homologue, hMyD88 associates with the death domains of the interleukin-1 receptor-associated kinases, the vertebrate homologue of Pelle, to form oligomeric assemblies,[3] a property similar to that observed in the PIDDosome, an activating complex for Caspase-2 (25). This suggests that in the *Drosophila* postreceptor pathway death domain complexes may be simpler oligomeric assemblies than those that mediate mammalian innate immune responses. On the other hand it is to be expected that

[3] P. Motshwene, M. C. Moncrieffe, and N. J. Gay unpublished data.

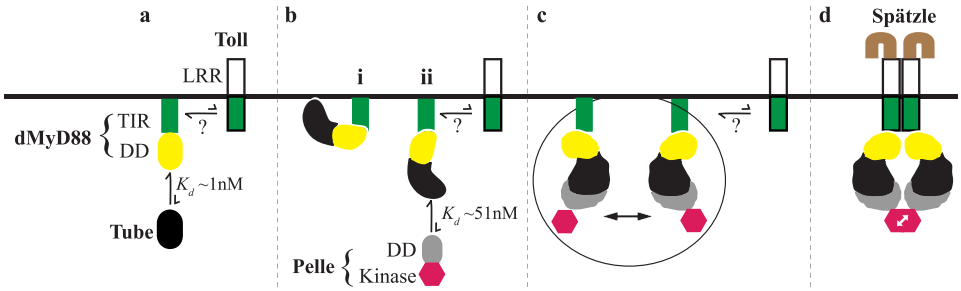

FIGURE 6. **Model of the postreceptor events in Toll signaling.** *a*, the death domain of dMyD88 interacts with the death domain of Tube to yield a high affinity ($K_d \approx 1$ nM) membrane-localized presignaling heterodimeric complex (the possibility for transient associations between the TIR domains of dMyD88 and Toll is also shown). The interaction between the death domains of dMyD88 and Tube is sufficient to produce a surface on Tube that enables a high affinity ($K_d \approx 51$ nM) interaction) with the death domain of Pelle *b*, *ii*, however, it is also possible that the Pelle binding site on Tube of the Tube-dMyD88 heterodimer is masked (*i*) preventing heterotrimer assembly. If a membrane-localized dMyD88-Tube-Pelle heterotrimeric complex is produced, its conformation and/or dynamics are such that dimerization and consequently transphosphorylation of the kinase domain of Pelle are prevented (*c*). Recent data (44) suggest that dimeric Spätzle does not cross-link the ectodomains of two Toll monomers, but instead two Spätzle dimers bind end-on to Toll and promote receptor dimerization and thus activation. Active Toll then either recruits the dMyD88-Tube-Pelle complex and locks them in a conformation that allows transphosphorylation of the kinase domain of Pelle and subsequent downstream events, or the dMyD88-Tube dimer, which now has the Pelle binding surface on Tube exposed, allows Pelle binding and transphosphorylation of the kinase domains. *LRR*, leucine-rich repeat.

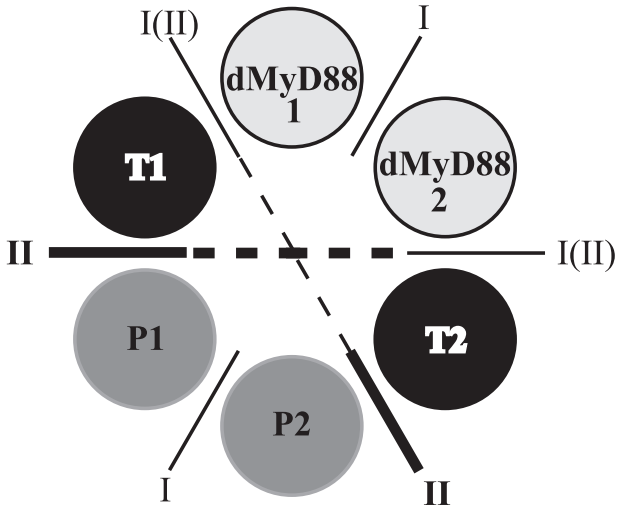

FIGURE 7. **Death domain interactions inferred by analogy with the PIDDosome core complex (25).** The active Toll complex is comprised of a hexameric array having two dMyD88-Tube-Pelle heterotrimers (dMyD88 1-T1-P1 and dMyD88 2-T2-P2). The dMyD88-Tube interface is either Type I or Type II, whereas the Pelle-Pelle (P1-P2) and dMyD88-dMyD88 (dMyD88 1-dMyD88 2) interfaces are likely Type I. A Type III surface is generated at the geometric center where Tube-Tube (T1:T2) contacts are possible.

two dMyD88-Tube heterodimers or dMyD88-Tube-Pelle heterotrimers will associate with each activated receptor complex, and this process of recruitment may display allosteric characteristics. Thus it is possible that stepwise assembly of the signaling complex promotes the formation of further homotypic interactions between the death domains of Pelle analogous to those seen in the PIDDosome (25) (Fig. 7). As shown, homotypic interactions between the death domains of dMyD88 and Pelle are possible. Interestingly if one assumes that the dMyD88-Tube interface is a Type I interface and that the Tube-Pelle interface is Type II as observed crystallographically, then a Type III interface is only generated at the geometric center where Tube-Tube contacts are likely to occur. Thus, the assembly of the signaling oligomeric death domain complex in *Drosophila*, unlike the PIDDosome, would appear to utilize predominantly only two types of interfaces, Type I and Type II.

The sedimentation coefficient values of the heterodimeric Tube-dMyD88 and the heterotrimeric Pelle-Tube-dMyD88 allow estimates of the shapes these complexes adopt in solution to be made by modeling them as prolate or oblate ellipsoids. Model selection is aided by comparing the dimensions of the long axis predicted from the sedimentation data with the SAXS-derived D_{max} values. This suggests that both the Tube-dMyD88 and the Pelle-Tube-dMyD88 complexes are best modeled as oblate ellipsoids. Shape reconstructions of the Pelle-Tube-dMyD88 DD trimer obtained from the SAXS data and the subsequent fitting of the known three-dimensional structure of the Pelle-Tube complex into this model has provided insights into how the constituent components are assembled. Our SAXS data are consistent with an almost linear death domain arrangement (in the form of a kidney-shaped complex), indicating that interactions between the monomer cores of the Pelle and dMyD88 death domains are unlikely.

Acknowledgments—We thank Dr. Peter Schuck for helpful discussions regarding the determination of K_d values from sedimentation equilibrium data and "wiz" for careful reading of the manuscript.

REFERENCES

1. Belvin, M. P., and Anderson, K. V. (1996) *Annu. Rev. Cell Dev. Biol.* **12,** 393–416
2. Hashimoto, C., Hudson, K. L., and Anderson, K. V. (1988) *Cell* **52,** 269–279
3. Weber, A. N. R., Tauszig-Delamasure, S., Hoffmann, J. A., Lelièvre, E., Gascan, H., Ray, K. P., Morse, M. A., Imler, J.-L., and Gay, N. J. (2003) *Nat. Immunol.* **4,** 794–800
4. Chasan, R., and Anderson, K. V. (1989) *Cell* **56,** 391–400
5. Jang, I.-H., Chosa, N., Kim, S.-H., Nam, H.-J., Lemaitre, B., Ochiai, M., Kambris, Z., Brun, S., Hashimoto, C., Ashida, M., Brey, P. T., and Lee, W.-J. (2006) *Dev. Cell* **10,** 45–55
6. Ray, R. P., Arora, K., Nüsslein-Volhard, C., and Gelbart, W. M. (1991) *Development* **113,** 35–54
7. Meng, X., Khanuja, B. S., and Ip, Y. T. (1999) *Genes Dev.* **13,** 792–797
8. Rutschmann, S., Jung, A. C., Hetru, C., Reichhart, J. M., Hoffmann, J. A., and Ferrandon, D. (2000) *Immunity* **12,** 569–580
9. Lee, M. S., and Kim, Y.-J. (2007) *Annu. Rev. Biochem.* **76,** 447–480
10. Sun, H., Bristow, B. N., Qu, G., and Wasserman, S. A. (2002) *Proc. Natl. Acad. Sci. U. S. A.* **99,** 12871–12876
11. Chen, L.-Y., Wang, J.-C., Hyvert, Y., Lin, H.-P., Perrimon, N., Imler, J.-L., and Hsu, J.-C. (2006) *Curr. Biol.* **16,** 1183–1193
12. Tauszig-Delamasure, S., Bilak, H., Capovilla, M., Hoffmann, J. A., and Imler, J.-L. (2002) *Nat. Immunol.* **3,** 91–97
13. Shelton, C. A., and Wasserman, S. A. (1993) *Cell* **72,** 515–525
14. Sun, H., Towb, P., Chiem, D. N., Foster, B. A., and Wasserman, S. A. (2004)

EMBO J. **23,** 100–110
15. Shen, B., and Manley, J. L. (1998) *Development* **125,** 4719–4728
16. Edwards, D. N., Towb, P., and Wasserman, S. A. (1997) *Development* **124,** 3855–3864
17. Drier, E. A., Huang, L. H., and Steward, R. (1999) *Genes Dev.* **13,** 556–568
18. Isoda, K., and Nüsslein-Volhard, C. (1994) *Proc. Natl. Acad. Sci. U. S. A.* **91,** 5350–5354
19. Shen, B., and Manley, J. L. (2002) *Development* **129,** 1925–1933
20. Huang, B., Eberstadt, M., Olejniczak, E. T., Meadows, R. P., and Fesik, S. W. (1996) *Nature* **384,** 638–641
21. Fesik, S. W. (2000) *Cell* **103,** 273–282
22. Xiao, T., Towb, P., Wasserman, S. A., and Sprang, S. R. (1999) *Cell* **99,** 545–555
23. Weber, C. H., and Vincenz, C. (2001a) *Trends Biochem. Sci.* **26,** 475–481
24. Weber, C. H., and Vincenz, C. (2001b) *FEBS Lett.* **492,** 171–176
25. Park, H. H., Logette, E., Raunser, S., Cuenin, S., Walz, T., Tschopp, J., and Wu, H. (2007) *Cell* **128,** 533–546
26. Schiffmann, D. A., White, J. H., Cooper, A., Nutley, M. A., Harding, S. E., Jumel, K., Solari, R., Ray, K. P., and Gay, N. J. (1999) *Biochemistry* **38,** 11722–11733
27. Moncrieffe, M. C., Stott, K. M., and Gay, N. J. (2005) *FEBS Lett.* **579,** 3920–3926
28. Edelhoch, H. (1967) *Biochemistry* **6,** 1948–1954
29. Vistica, J., Dam, J., Balbo, A., Yikilmaz, E., Mariuzza, R. A., Rouault, T. A., and Schuck, P. (2004) *Anal. Biochem.* **326,** 234–256
30. Schuck, P. (2000) *Biophys. J.* **78,** 1606–1619
31. Houtman, J. C. D., Brown, P. H., Bowden, B., Yamaguchi, H., Appella, E., Samelson, L. E., and Schuck, P. (2007) *Protein Sci.* **16,** 30–42
32. Svergun, D. (1992) *J. Appl. Crystallogr.* **25,** 495–503
33. Svergun, D. I., Petoukhov, M. V., and Koch, M. H. (2001) *Biophys. J.* **80,** 2946–2953
34. Volkov, V., and Svergun, D. (2003) *J. Appl. Crystallogr.* **36,** 860–864
35. Kozin, M. B., and Svergun, D. I. (2001) *J. Appl. Crystallogr.* **34,** 9
36. Chacón, P., and Wriggers, W. (2002) *J. Mol. Biol.* **317,** 375–384
37. Wriggers, W., and Chacon, P. (2001) *J. Appl. Crystallogr.* **34,** 773–776
38. Horng, T., and Medzhitov, R. (2001) *Proc. Natl. Acad. Sci. U. S. A.* **98,** 12654–12658
39. Brown, P. H., and Schuck, P. (2006) *Biophys. J.* **90,** 4651–4661
40. Gay, N. J., and Gangloff, M. (2007) *Annu. Rev. Biochem.* **76,** 141–165
41. Rowe, D. C., McGettrick, A. F., Latz, E., Monks, B. G., Gay, N. J., Yamamoto, M., Akira, S., O'Neill, L. A., Fitzgerald, K. A., and Golenbock, D. T. (2006) *Proc. Natl. Acad. Sci. U. S. A.* **103,** 6299–6304
42. Kagan, J. C., and Medzhitov, R. (2006) *Cell* **125,** 943–955
43. Kagan, J. C., Su, T., Horng, T., Chow, A., Akira, S., and Medzhitov, R. (2008) *Nat. Immunol.* **9,** 361–368
44. Gangloff, M., Murali, A., Xiong, J., Arnot, C. J., Weber, A. N., Sandercock, A. M., Robinson, C. V., Sarisky, R., Holzenburg, A., Kao, C., and Gay, N. J. (2008) *J. Biol. Chem.* **283,** 14629–14635